

RESEARCH

Open Access



Upper respiratory tract microbiota is associated with small airway function and asthma severity

Yi Li¹, Congying Zou², Jieying Li³, Wen Wang^{3*}, Yue Guo³, Lifang Zhao³, Chunguo Jiang³, Peng Zhao⁴ and Xingqin An¹

Abstract

Background Characteristics of airway microbiota might influence asthma status or asthma phenotype. Identifying the airway microbiome can help to investigate its role in the development of asthma phenotypes or small airway function.

Methods Bacterial microbiota profiles were analyzed in induced sputum from 31 asthma patients and 12 healthy individuals from Beijing, China. Associations between small airway function and airway microbiomes were examined.

Results Composition of sputum microbiota significantly changed with small airway function in asthma patients. Two microbiome-driven clusters were identified and characterized by small airway function and taxa that had linear relationship with small airway functions were identified.

Conclusions Our findings confirm that airway microbiota was associated with small airway function in asthma patients.

Keywords Asthma, Microbiome, Phenotype, Small airway function, Maximal expiratory flow

Background

Asthma is a heterogeneous disease characterized by inflammation and hyperresponsive in airways, which has several phenotypes and endotypes that may response differently to therapies. Despite important advances in

asthma, including greater awareness, timely diagnosis, and pharmacological interventions targeted at airway inflammation, control of asthma in patients remains unsatisfactory.

A possible reason for poor asthma control might be that other than “Eosinophils asthma phenotype” or “Neutrophil asthma phenotype”, some patients express a “small airways phenotype”, which has small airways inflammation and dysfunction that is not being targeted or controlled by current therapies. The small airways are defined by an internal airway diameter of <2 mm. They have a generation number that is generally higher than 8, and they account for 98.8% (approximately 4500 ml) of the total lung volume, compared to that the large airways account for only 1.2% (approximately 50 ml). Though inflammation and remodeling in asthma involve the large airways, the small airways are the major site of airflow

*Correspondence:

Wen Wang
wenwang_doc@126.com

¹ State Key Laboratory of Severe Weather of CMA, Chinese Academy of Meteorological Sciences, Beijing 100081, China

² Department of Surgery, Beijing ChaoYang Hospital, Capital Medical University, Chaoyang District, Beijing, China

³ Department of Respiratory and Critical Care Medicine, Beijing Institute of Respiratory Medicine and Beijing Chao-Yang Hospital, Capital Medical University, No.8, Gongtitan Road, Chaoyang District, Beijing 100020, China

⁴ Department of Health and Environmental Sciences, Xi'an Jiaotong-Liverpool University, Suzhou, China



limitation, and where the intensity of the inflammation may be even higher than that in large airways. Trans-bronchial biopsy findings show that small airways are the major site of inflammation and contain immunocytes that putatively account for the tissue remodeling noted [1, 2]. Thus, small airways might affect the pathobiology of asthma and small airway dysfunction may contribute to poor asthma control [1–4], and the small airways of individuals with asthma are increasingly recognized as a potential therapeutic target [2, 4, 5].

The microbiota in human airways changes with disease. With the bacterial 16S ribosomal RNA gene sequencing technique, different microbiota were identified between asthma phenotypes, suggesting that microbial patterns in the airways may influence distinct phenotypes of asthma [6–8] and allergic inflammation [9]. Airway microbiota composition is also associated with the degree of airway hyperresponsiveness among patients with less controlled asthma. Indeed, several bacterial taxa, including *Streptococcus pneumoniae*, *Staphylococcus aureus*, *Moraxella catarrhalis*, *Pseudomonas aeruginosa*, and *Haemophilus influenzae*, were reported to be associated with asthma exacerbation or development [10, 11]. Moreover, studies suggest that airway microbiome in asthma patients is probably a result of complex interactions between the inflammatory milieu and the drug effects, and microbial-derived mechanisms might be the reason of poor response to the treatment. For example, treatment with a combination of inhaled corticosteroids (ICSs) and oral glucocorticoids correlates positively with an increased abundance of *Proteobacteria* and *Pseudomonas*, and with a decreased abundance of *Bacteroidetes*, *Fusobacteria*, and *Prevotella* [12]. Meanwhile, a unique enrichment of *Haemophilus*, *Neisseria*, *Fusobacterium*, *Porphyromonas* species and the *Sphingomonadaceae* family along with depletion in *Mogibacteriaceae* and *Lactobacillales* was observed in mild asthma patients without being treated with ICSs [13].

In this study, the association between airway microbiota pattern and small airway function was explored. Results from lung function tests were related to the bacterial flora in study subject sputum.

Methods

Pulmonary function measurements

The measurements of spirometry function were conducted by Jaeger Masterscreen PFT (Viasys Healthcare, Höchberg, Germany) according to the recommendations of the *Chinese National Guidelines of Pulmonary Function Test* [14]. Following indices were used to characterize small airway function: forced expiratory volume in first second (FEV1), forced expiratory vital capacity (FVC), peak expiratory flow (PEF), maximal expiratory flow at

25% vital capacity (MEF25), maximal expiratory flow at 50% vital capacity (MEF50), percentage of tested MEF25 to predicted MEF25 ($\text{MEF25}_{\text{pred}\%}$), percentage of tested MEF50 to predicted MEF50 ($\text{MEF50}_{\text{pred}\%}$) and forced expiratory flow between 25 and 75% (MEF (75/25)).

Study population

All individuals with asthma were patients from the Respiratory Department in Chaoyang Hospital, Beijing, while 12 healthy individuals were recruited from routine physical examination department in the same institution. The age distribution of these healthy people were from 28 to 58 and they were ruled out of asthma and other respiratory diseases by scan examination and pulmonary function tests according to the *Global Strategy for Asthma Management and Prevention* [15, 16].

Among the 31 individuals with asthma, we took a cut-off value of 65% for $\text{MEF25}_{\text{pred}\%}$ and $\text{MEF50}_{\text{pred}\%}$ to define study groups according to the Chinese Thoracic Society [17–19]. We defined patients who had a $\text{MEF25}_{\text{pred}\%}$ lower than 65% as the $\text{MEF25}_{\text{pred}\%}$ -low group (26 people), and others with a $\text{MEF25}_{\text{pred}\%}$ value higher than 65% as the $\text{MEF25}_{\text{pred}\%}$ -high group (5 people). The $\text{MEF50}_{\text{pred}\%}$ -low group and $\text{MEF50}_{\text{pred}\%}$ -high group were similarly defined, and 14 patients were grouped in the $\text{MEF50}_{\text{pred}\%}$ -high group versus 17 in the $\text{MEF50}_{\text{pred}\%}$ -low group.

As MEF50 and MEF25 are similar indices of small airway function, and because the sample size of the $\text{MEF50}_{\text{pred}\%}$ -high group and $\text{MEF50}_{\text{pred}\%}$ -low group is closer than those of $\text{MEF25}_{\text{pred}\%}$ groups, we compared the sputum microbiome only between the MEF50 groups and the healthy individuals.

Subject characteristics are presented in Table 1.

Sampling of induced sputum

Induced sputum from asthma patients and health individuals was collected according to standardized protocols [20, 21]. Study subjects were pre-treated with inhaled salbutamol to relax airway smooth muscle and to prevent acute asthma attack. Then they inhaled a nebulized solution of 3% saline over a 2-minute period, spat out the saliva, took 2 deep inspirations of saline, and coughed sputum into a separate cup. This procedure was repeated for six times. Subjects were instructed to rinse orally with water and to blow their nose after each inhalation to avoid contamination with saliva and post-nasal drip. Sputum samples were collected into sterilized pots and stored at -80°C for bacterial DNA extraction. Peak flow is monitored throughout the procedure, if patients feel uncomfortable or symptoms occurred, the induction was stopped.

Table 1 Clinical characteristics of study subjects^a

	MEF _{25pred%}		MEF _{50pred%}	
	high	low	high	low
Subject(n)	5	26	14	17
Age	34.40 ± 16.20	46.34 ± 12.83	41.35 ± 14.72	46.94 ± 13.00
Male (%)	60	54	57	47
Atopy (%)	100	85	90	84
BMI [#]	24.61 ± 5.66	26.74 ± 4.54	25.43 ± 4.12	27.19 ± 5.11
MEF25	(1.9 ± 0.81)*	(0.69 ± 0.36)*	(1.34 ± 0.65)**	(0.51 ± 0.29)**
MEF50	(4.33 ± 1.32)*	(2.19 ± 1.16)*	(3.73 ± 1.05)**	(1.55 ± 0.74)**
MEF75	(8.02 ± 2.45)*	(4.49 ± 2.25)*	(7.22 ± 1.86)**	(3.28 ± 1.54)**
MEF(75/25)	(3.85 ± 1.28)*	(1.7 ± 0.89)*	(3.06 ± 1.02)**	(1.22 ± 0.62)**
FeNO (ppb)	(24.8 ± 12.38)*	(41.32 ± 24.66)*	30.86 ± 14.44	45.31 ± 28.38
IgE(ng·mL ⁻¹) ^b	148.9 ± 71.55	326.48 ± 393.57	277.93 ± 430.54	319.11 ± 340.12
Neutrophil ^b (× 10 ⁹ /L)	(3.27 ± 0.32)**	(5.06 ± 1.40)**	4.29 ± 1.71	5.16 ± 1.21
Eosinophils ^b (× 10 ⁹ /L)	0.34 ± 0.33	0.51 ± 0.65	0.31 ± 0.28	0.59 ± 0.74
ACT score	23 ± 2.65	21.43 ± 3.81	23 ± 1.89	20.75 ± 4.3
AQLQ score	82.67 ± 17.5	88.27 ± 15.1	90.2 ± 12.4	85.87 ± 16.88
VC	4.18 ± 0.75	3.66 ± 0.97	(4.13 ± 0.75)*	(3.43 ± 0.99)*
FVC	4.15 ± 0.75	3.64 ± 0.98	(4.11 ± 0.76)*	(3.42 ± 1.01)*
FEV1	(3.58 ± 0.75)*	(2.51 ± 0.85)*	(3.32 ± 0.66)**	(2.15 ± 0.75)**
FEV1/FVC	(102.88 ± 7.78)**	(81.12 ± 13.07)**	(97.01 ± 6.52)**	(74.45 ± 11.3)**
PEF	8.98 ± 2.07	7.01 ± 2.21	(8.71 ± 1.96)**	(6.17 ± 1.87)**

^a Data are expressed as mean values and standard errors^b counts in blood*: indicating a statistical significant difference between MEF25_{pred%}-high and MEF25_{pred%}-low groups, or between MEF50_{pred%}-high and MEF50_{pred%}-low groups.Significant level: *, $p < 0.05$; **, $p < 0.01$

DNA extraction, PCR amplification and Illumina sequencing

Microbial DNA was extracted from induced sputum. The final DNA concentration and purification were determined by NanoDrop 2000 UV-vis spectrophotometer (Thermo Scientific, Wilmington, USA), and DNA quality was checked by 1% agarose gel electrophoresis. The V3-V4 hypervariable regions of the bacteria 16S rRNA gene were amplified with primers 338F (5'-ACTCCTACGGGAGGCAGCAG-3') and 806R (5'-GGACTA CHVGGGTWCTCTAAT-3') by thermocycler PCR system (GeneAmp 9700, ABI, USA). The PCR reactions were conducted using the following program: 3 min of denaturation at 95°C, 27 cycles of 30 s at 95°C, 30 s for annealing at 55°C, and 45 s for elongation at 72°C, and a final extension at 72°C for 10 min. PCR reactions were performed in triplicate 20 µL mixture containing 4 µL of 5 × FastPfu Buffer, 2 µL of 2.5 mM dNTPs, 0.8 µL of each primer (5 µM), 0.4 µL of FastPfu Polymerase and 10 ng of template DNA. The resulted PCR products were extracted from a 2% agarose gel and further purified using the AxyPrep DNA Gel Extraction Kit (Axygen Biosciences, Union City, CA, USA) and quantified using

QuantiFluor™-ST (Promega, USA) according to the manufacturer's protocol.

Purified amplicons were pooled in equimolar and paired-end sequenced (2 × 300) on an Illumina MiSeq platform (Illumina, San Diego, USA) according to the standard protocols [22, 23].

Bioinformatics analysis

The analysis was conducted by following the "Atacama soil microbiome tutorial" of Qiime2docs along with customized program scripts (<https://docs.qiime2.org/2019.1/>). Briefly, raw data FASTQ files were imported into the format which could be operated by QIIME2 system using qiime tools import program. Demultiplexed sequences from each sample were quality filtered and trimmed, de-noised, merged, and then the chimeric sequences were identified and removed using the QIIME2 dada2 plugin to obtain the feature table of amplicon sequence variant (ASV). The QIIME2 feature-classifier plugin was then used to align ASV sequences to a pre-trained GREENGENES 13_8 99% database (trimmed to the V3V4 region bound by the 338F/806R primer pair) to generate the taxonomy table. Any

contaminating mitochondrial and chloroplast sequences were filtered using the QIIME2 feature-table plugin.

Experimental materials and reagents are included in supplementary material (suppl. Table 1).

Statistics and identification of bacterial communities

We used a rank test method, the Kruskal–Wallis test to examine the differences between groups. The linear Discriminant Analysis Effect Size (LEfSe) method [24] was employed to compare the bacterial composition between groups, with the cutoff p -value set as 0.05 (after Benjamini-Hochberg false discovery rate correction). Additionally, Kyoto Encyclopedia of Genes and Genomes (KEGG) functional profiles of microbial communities were predicted with Phylogenetic Reconstruction of Unobserved States (PICRUST) [25].

Microbiome Multivariable Associations with Linear Models (MaAsLins) were run to test for associations between microbiomes and clinical variables using the MaAsLin 2 R/Bioconductor software package [26, 27]. The linear mixed-effect model could be expressed as follows:

$$\text{Bacterial taxon} \sim (\text{intercept}) + \text{small airway index} + (1 / \text{subject}).$$

All analyses were performed using R studio (version 1.1.453) [28] with R software (version 3.5.1) [29] supported with the following software packages: vegan, metacoder [30], MaAsLin2 [27], ggplot2, Tax4Fun2 [31], and mixOmics [32].

Results

Clinical characteristics of the study subjects

Clinical features of the subjects are shown in Table 1, all significantly ($p < 0.05$) different indices between MEF25_{pred%}-high group and MEF25_{pred%}-low group or between MEF50_{pred%}-high group and MEF50_{pred%}-low group were marked with a “*”. As expected, FEV₁, FEV₁/FEC, MEF25, MEF50, MEF75 and MEF (75/25) values were significantly ($p < 0.05$) lower in MEF25_{pred%}-low group than those in MEF25_{pred%}-high group, meanwhile neutrophil and Fractional exhaled nitric oxide (FeNO) were significantly ($p < 0.05$) higher in MEF25_{pred%}-low group than those in MEF25_{pred%}-high group. VC, PEF, FEV₁, FEV₁/FEC, MEF25, MEF50, MEF75 and MEF (75/25) values were significantly ($p < 0.05$) lower in MEF50_{pred%}-low group than those in MEF50_{pred%}-high group. Associations between these significantly different indices and microbiome were investigated by MaSLin2 (in later sections).

No significant difference of blood eosinophils or serum IgE was observed between these two pairs of groups.

Sputum microbiome compositions

A total of 2,305,983 valid reads were generated for the 43 samples. After filtering for low-quality reads, 51,245 sequence reads were used for subsequent analyses and resulted in 12,265 OTUs. The average percentage of input passed filter was approximately 85%, and average percentage of input non-chimeric was approximately 77%.

We first examined the sputum microbiome composition. Taxa barplots and pie chart of bacterial genera in healthy control subjects and MEF50_{pred%}-low group are presented in Fig. 1A, B and C. At the genus level, the top five genera of the healthy control sputum microbiome were *Prevotella* (19.57%), *Veillonella* (9.74%), *Neisseria* (6.80%), *Streptococcus* (5.63%), *Porphyromonas* (3.30%). The top five genera of MEF50_{pred%}-low group was *Prevotella* (12.86%), *Streptococcus* (10.24%), *Veillonella* (9.27%), *Fusobacterium* (4.18%) and *Neisseria* (3.43%).

We then compared the difference in the median relative abundance of taxa between the healthy individuals and MEF50_{pred%}-low group, as the metagenomics phylogenetic map shows in Fig. 1D.

It could be seen from Fig. 1D that the largest significant ($p < 0.05$) difference in the median relative abundance of taxa was observed in the genus *Prevotella*, which was in accordance with the difference in microbiome composition. At the species level in this genus, significant ($p < 0.05$) difference was observed in species *Prevotella nanceiensis* (*P. nanceiensis*), *Prevotella nigrescens* (*P. nigrescens*), *Prevotella copri* (*P. copri*) and *Prevotella pallens* (*P. pallens*), and all these species had a relative abundance higher than 0.01% (Supplementary Fig. 1).

The second largest significant ($p < 0.05$) difference in the median relative abundance of taxa was observed in genus *Streptococcus*. At the species level in this genus, the relative abundance of *Streptococcus infantis* (*S. infantis*) was significantly different between MEF50_{pred%}-low group and healthy control group (Supplementary Fig. 1).

Other species that had significant ($p < 0.05$) difference in relative abundance between MEF50_{pred%}-low group and the healthy controls include *Campylobacter rectus*

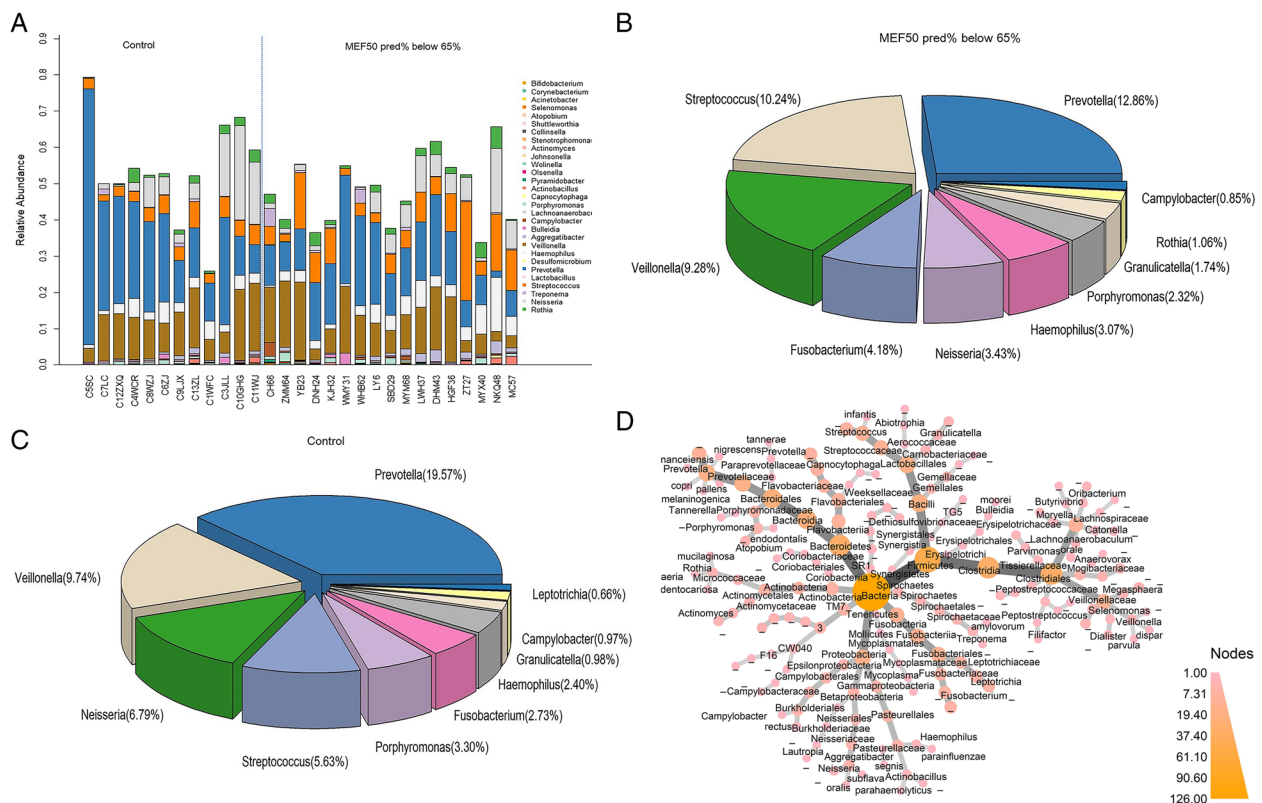


Fig. 1 The sputum microbiome at the genus level. **A** Bar plot of all the samples, each bar shows the relative abundance of one individual **B** Pie chart of the microbiome composition at genus level in MEF50_{pred%}-low group. **C** Pie chart of the microbiome composition at genus level in healthy individuals. **D** Phylogenetic map of the median relative abundance differences in bacterial taxa between the healthy control group and the MEF50_{pred%}-low group, the ending circle of each branch represented for species ($n = 29$). The depth of color of the nodes corresponds to the degree of difference in median relative abundance of the bacterial taxa. The darker the color of the phylogenetic branches, the higher median differences, whereas gray nodes and branches indicate no significant differences

(*C. rectus*) and *Collinsella aerofaciens* (*C. aerofaciens*) (Supplementary Fig. 1).

Partial least squares discriminant analysis (PLS-DA) of microbial difference

The PLS-DA model was established to identify the contribution of taxa to the difference in the community structure between the groups. Figure 2 shows the results of supervised PLS-DA plots concerning the microbial difference between MEF25_{pred%} and MEF50_{pred%} functional groups. It could be seen that the two clusters were characterized by composition difference according to MEF25_{pred%} (Fig. 2A), MEF50_{pred%} (Fig. 2B) function and asthma severity.

Moreover, a heat map of the Euclidian distance of taxa between clusters characterized by MEF50_{pred%} function groups was shown in Fig. 3, indicating the distribution of taxa to component 1 in each sample.

It could be seen that in the MEF50_{pred%}-low group, at the species level, *Johnsonella ignava*, *Rothia dentocariosa*

(*R. dentocariosa*), *C. rectus*, *Treponema socranskii* (*T. socranskii*), *P. nigrescens*, *Treponema amylovorum*, *Aggregatibacter segnis* (*A. segnis*), and *Corynebacterium durum* had the largest Euclidian distance between the two clusters. Meanwhile, in the MEF50_{pred%}-high group, *Veillonella dispar*, *P. pallens*, *P. nanceiensis*, and *P. melaninogenica* had the largest Euclidian distance between the two clusters.

Linear associations between sputum microbiome and small airway indices

Mixed multiple linear regression analysis (MaAslin) was performed to explore whether there was a linear relationship between sputum microbiomes with MEF25, MEF50, MEF75, PEF, MEF (75/25), and FEV₁/FVC. Figure 4 shows the heat map of these significant ($p < 0.05$) estimates, indicating the magnitude of coefficients in the linear associations.

It could be seen that MEF (75/25) and FEV₁/FVC had most associations with the microbiome. Only

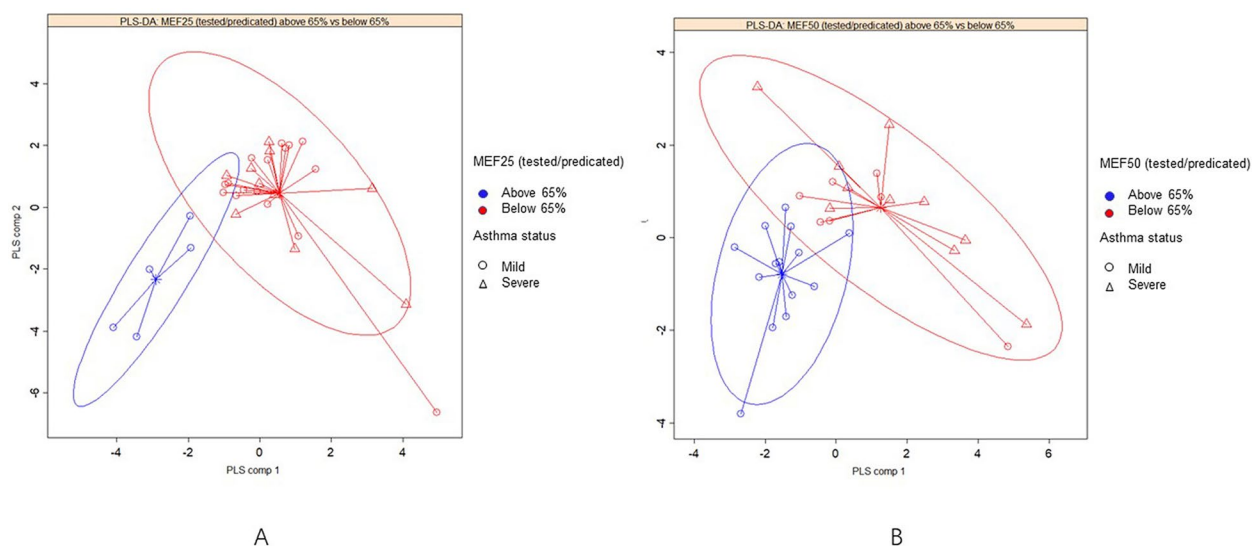


Fig. 2 Supervised PLS-DA plots with confidence ellipse, arrows point to the outcome category of each subject, including mild asthma and severe asthma as a subgroup. **A** MEF25_{pred%} group with a subgroup of asthma status. **B** MEF50_{pred%} group with a subgroup of asthma status

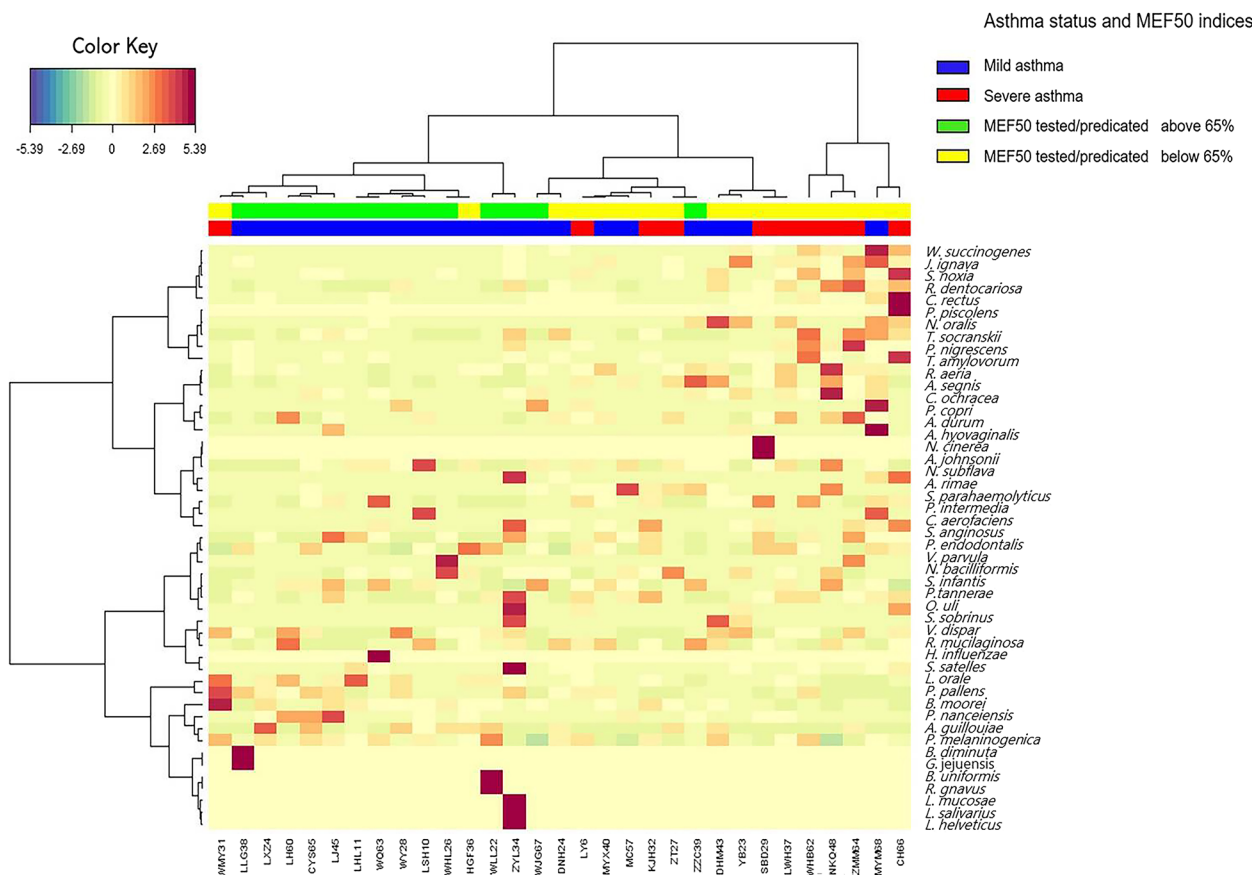


Fig. 3 Clustered image maps by different MEF50_{pred%} groups, including asthma status as a subgroup. Samples are represented in columns and taxa in rows. The colored side at the top of the heatmap indicates different groups. (Note: this plot was created with package mixOmics [32] of R software (version 3.5.1) [29])

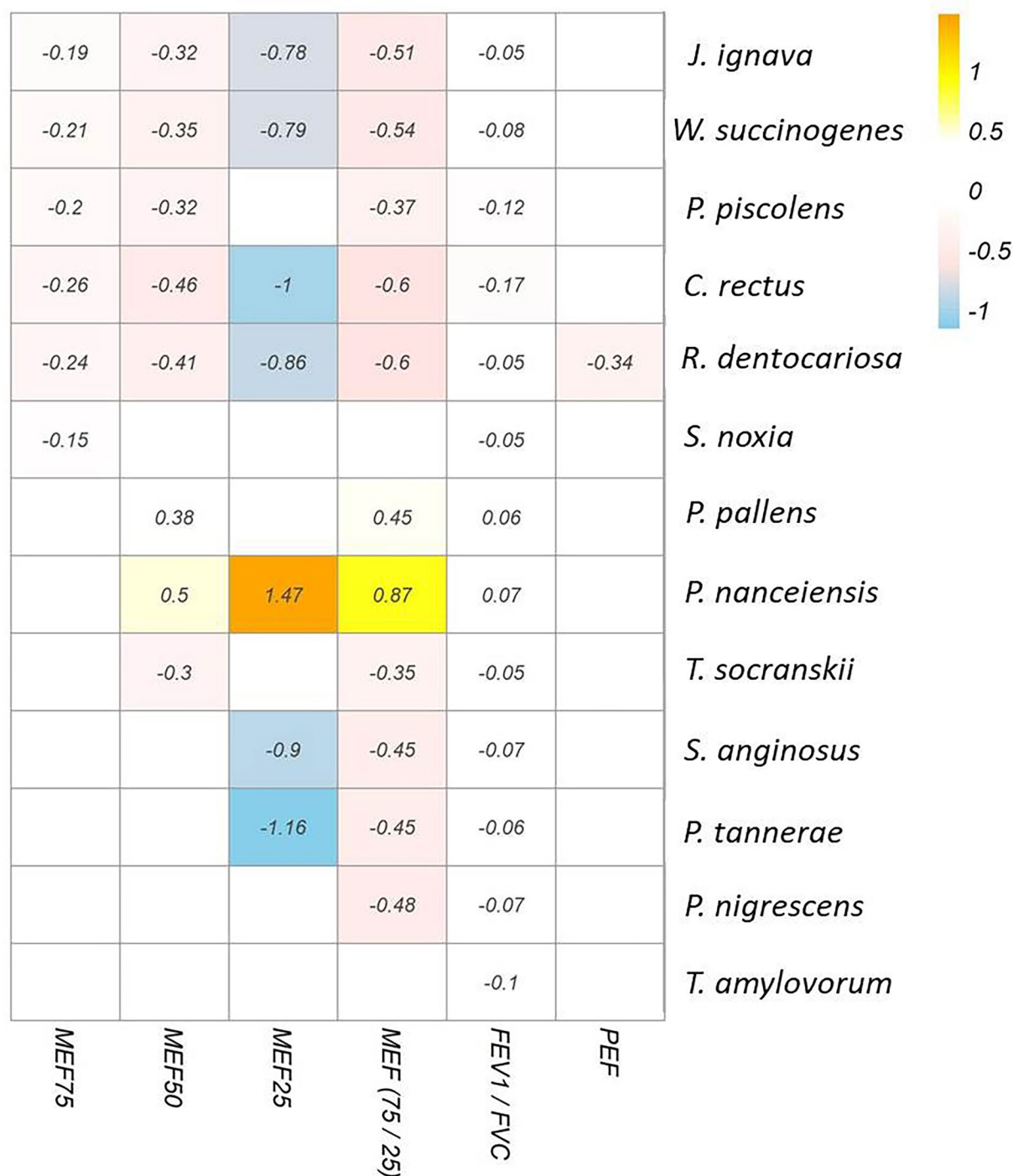
Significant associations($-\log(qval)*\text{sign}(coeff)$)

Fig. 4 MaAslin analysis of the heat map between small airway indices and microbiome. Only significant ($p < 0.05$) associations are shown. The numbers in the figure indicate the magnitude of coefficients in the linear associations

two species, *P. nanceiensis* and *P. pallens*, had positive associations with MEF25, MEF50, MEF (75/25), and FEV₁/FVC levels, whereas the species *J. ignava*, *R. dentocariosa*, *W. succinogenes*, and *C. rectus* had

negative associations with the three MEF indices. The species *P. piscocolens* had a negative association with MEF25, MEF50, MEF (75/25), and FEV₁/FVC levels. The species *Selenomonas noxia* had a negative

association with MEF75 and FEV₁/FVC, while the species *T. socranskii* had a negative association with MEF50, MEF75/25, and FEV₁/FVC. Lastly, the species *Streptococcus. anginosus* and *Prevotella tannerae* had negative associations with MEF25, MEF75/25, and FEV₁/FVC.

KEGG pathway analysis

16S rDNA amplicon data were supplemented with genomic data using PICRUSt. Genes from different bacteria likely to perform the same function have been grouped into KEGG orthologues (KO) by the Kyoto Encyclopedia of Genes and Genomes (KEGG). Differentially abundant KOs were screened by using the Bonferroni-corrected Wilcoxon rank sum test for differences between healthy individuals and MEF50_{pred%}-low group. Significant ($p < 0.05$) differences are shown in Fig. 5. In the MEF25_{pred%}-low and MEF25_{pred%}-high groups, changes in the microbial flora of function genes in six categories were related to pathways associated with metabolism of cofactors and vitamins, transport and catabolism, biosynthesis and secondary metabolism, immune disease, and the endocrine system (Fig. 5A). For the MEF50_{pred%}-low and MEF50_{pred%}-high groups, changes in the function genes were in genes associated with energy and carbohydrate metabolism, replication and repair, protein folding, sorting and degradation, amino acid metabolism, drug resistance, xenobiotics, and infectious disease (Fig. 5B).

Discussion

In this study, we found significant differences in the composition, relative abundance, biomarkers and signaling pathways of airway microbiome between small airway functional groups and healthy controls. Two microbiome-driven clusters were identified and characterized by small airway function, and change in the microbiome composition between small airway functional group was observed. Our study gave evidence to the connection between respiratory tract microbiota and small airway function in asthma patients.

Although the precise role of bacterium in airway inflammation remains to be established, some genera or bacteria were reported to be associated with asthma severity and phenotype. Specifically, genera *Haemophilus*, *Moraxella*, and *Neisseria* of the phylum *Proteobacteria*, or species *Haemophilus influenzae* and *Moraxella catarrha*, were associated with worse asthma control [6, 8, 33, 34]. In this study, we also found some associations between specific bacteria and small airway functions. First, we observed two species, *P. pallens* and *P. nanceiensis*, were correlated with better small airway function and better asthma status.

These two species had positive linear estimates with MEF50, MEF25, MEF (75/25) and FEV₁/FVC. More than that, *P. nanceiensis* was a biomarker in the healthy control group (Supplementary Fig. 2), and its relative abundance significantly ($p < 0.05$) decreased in small airway dysfunction groups (MEF25_{pred%}-low and MEF50_{pred%}-low groups); and it had the largest decreased fold-difference in MEF50_{pred%}-low group

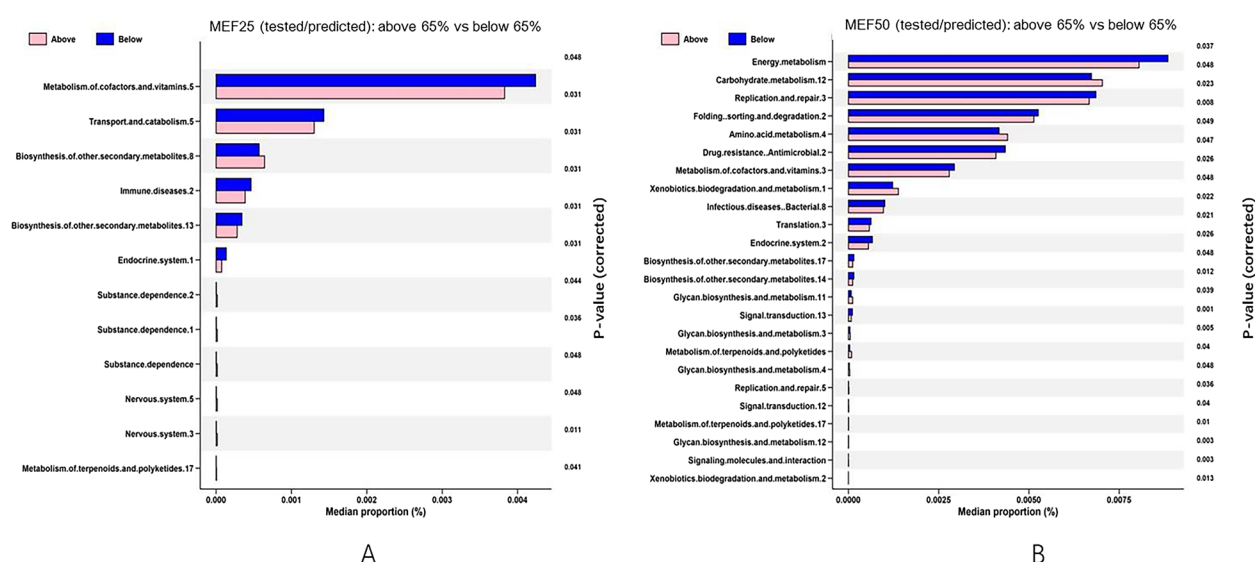


Fig. 5 KEGG pathway analysis between the study groups. **A** MEF25_{pred%}-low and MEF25_{pred%}-high groups. **B** MEF50_{pred%}-low and MEF50_{pred%}-high groups. (Note: all the KEGG identifiers were from <https://www.kegg.jp/kegg/>)

(Supplementary Fig. 3). This is in accordance with those studies that reported *P. nanceiensis* as a “beneficial” commensal bacterium in respiratory system. In one of those studies, compared with healthy airways, abundance of *P. nanceiensis* decreased in the airways of patients with chronic obstructive pulmonary disease (COPD), asthma, diabetes, celiac disease, and chronic periodontitis [35, 36]. In another study about children with Henoch-Schönlein Purpura [37], *P. nanceiensis* was observed to be positively correlated with IgA increase. IgA is important at mucosal surfaces for maintaining homeostasis [38, 39], and it complexes activate eosinophils and neutrophils in inflammation. In this situation, *P. nanceiensis* might have participated in the immune responses. This is in accordance with earlier findings that increased *P. nanceiensis* was associated with diminished neutrophilic airway inflammation, suggesting that *P. nanceiensis* is related to Th2-high type asthma [40]. So it is possible that some commensal bacteria of the airways may participate in the regulation of local and distant immune responses [41].

We also observed that some taxa that had negative associations with small airway functions or enriched significantly ($p < 0.05$) in MEF25_{pred%}-low or MEF50_{pred%}-low group. Many of these taxa play a role in human lung, oral and cardiovascular diseases [42]. Among these taxa, *C. rectus*, which had the largest negative estimate with all small airway functional indices, was enriched significantly ($p < 0.05$) in MEF25_{pred%}-low and MEF50_{pred%}-low groups. *C. rectus* was reported to be associated with periodontal disease [43], and was linked to coronary artery disease, lung abscess, empyema, brain abscess, and osteomyelitis [43, 44]. The precise reasons for these associations are unclear. However, evidence showed that *C. rectus* increased production of the proinflammatory cytokines IL-6 and IL-8 in human gingival fibroblasts [45], suggesting it may induce an inflammatory milieu in other tissues.

In this study, *P. nigrescens* was also observed to have a negative estimate with MEF (75/25) and FEV₁/FVC. More recently, *P. nigrescens* was reported to be associated with signs of carotid atherosclerosis in patients without periodontitis and endodontic infections [46, 47]. The later finding of dental colonization suggests possible distal spread of either the bacteria or inflammatory mediators such as cytokines. Still, patients with asthma show increased risk of bacterial infection. Certain bacterial species may transition from benign to pathogenic activities under some conditions but whether this is true in asthma requires additional research.

R. dentocariosa was the only taxa that had negative estimates with all small airway and lung functions observed in this study. *R. dentocariosa* is a normal commensal

bacterium of the oral cavity and is associated with dental caries and periodontal disease. The bacterium is also reported to be associated with septic arthritis, pneumonia, arteriovenous infection, and acute bronchitis [48]. Of note, *R. dentocariosa* can upregulation production of TNF- α by T cells [49].

S. anginosus was another taxa observed in our study to have a negative relationship with small airway function and it has been reported to be associated with pharyngitis and infections of internal organs and certain body fluids [50].

Functional analysis using PICRUSt showed clear differences between the bacterial predicted metabolic functions in different study group in our work. Pathway analysis of changes in the microbial flora genes indicated that they were related to carbohydrate and amino acid metabolism, cellular processes, and human diseases, and that the changes were distributed in different proportions. These findings are in accordance with other reports and suggest increased metabolic activity of the airway microbiome in asthmatic individuals [51, 52]. However, due to the limitation of PICRUSt, this prediction did not correspond to specific genera. Combining these analytic approaches may yield new insights.

The present study has a number of limitations. First, the cohort sample size is moderate and may not accurately reflect the true population. Second, some important indexes, such as IgA, were not tested for all patients with asthma. Further, the role of seasonal irritants, pollutants and smoke ingestion, such as from tobacco, was not tested in this study.

To sum up, our work gave evidence that small airway function was associated with respiratory tract microbiome, and commensal microorganisms may participate in the regulation of local and distant immune responses. Our findings could provide some information to therapy for patients with “small airway phenotype” asthma.

Abbreviations

ACQ6	Asthma Control Questionnaire 6
BMI	Body Mass Index
GINA	Global Initiative for Asthma
FeNO	Fractional Exhaled Nitric Oxide
FEV1	Forced Expiratory Volume in 1 s
FVC	Forced Vital Capacity
MEF25	Maximal Expiratory Flow in 25% Vital Capacity
MEF50	Maximal Expiratory Flow in 50% Vital Capacity
MEF75	Maximal Expiratory Flow in 75% Vital Capacity
MEF _{25pred%}	Percentage of Tested MEF25 of Predicted MEF25
MEF50 _{pred%}	Percentage of Tested MEF50 of Predicted MEF50.
PCA	Principal Component Analysis
PEF	Peak Expiratory Flow Rate
KEGG	Kyoto Encyclopedia of Genes and Genomes
LEfSe	Linear Discriminant Analysis Effect Size method
PLS-DA	Partial Least Squares Discriminant Analysis
PICRUSt	Phylogenetic Investigation of Communities by Reconstruction of Unobserved States
VC	Vital capacity

Supplementary Information

The online version contains supplementary material available at <https://doi.org/10.1186/s12866-023-02757-5>.

Additional file 1: Sup. Table 1. Experimental materials and reagents. **Sup. Figure 1.** Differences between MEF50 function groups in microbiome composition at species level. **Sup. Figure 2.** Taxonomy tree and LDA scores of the groups. (A) Taxonomy tree and LDA scores between MEF50predicted%-low and MEF50predicted%-high groups. (B) Taxonomy tree and LDA scores between the MEF50predicted%-low group and the healthy control group. Circles from within to outward indicate the classification from the phylum to the genus, respectively. Each small circle represents a taxon with its diameter proportional to the relative abundance. Dots with different colors denote the core species of each group. Histogram showing the LDA scores of the biomarkers with statistical differences. **Sup. Figure 3.** Volcano plot of fold change (≥ 1.2 -fold, adjusted $p < 0.05$) between the MEF₅₀predicted%-low and MEF₅₀predicted%-high groups in subjects with asthma.

Acknowledgements

We thank Ms. Wu Xu for helping to collect the sputum samples.

Authors' contributions

Yi Li: data analysis and manuscript writing; Congying Zou: administrative support; Jieying Li: recording and interpretation of clinic metadata; Yue Guo: recording and interpretation of blood cell count data; Lifang Zhao: interpretation of lung function test result; Chunguo Jiang: interpretation of blood cell count data; Wen Wang: Conception and design; Peng Zhao: R software support; Xingqin An: R software support. The author(s) read and approved the final manuscript.

Funding

Natural Science Foundation of Beijing Municipality (No. 7192069) and the National Natural Science Foundation of China (grant no. 42175184).

Availability of data and materials

The 16S RNA datasets generated and analyzed during the current study are now accessible in the NCBI repository: <https://www.ncbi.nlm.nih.gov/bioproject/PRJNA879958>.

Declarations

Ethics approval and consent to participate

The study was approved by the Ethics Committee of the Chaoyang Hospital (ethics NO.2020-Re-425 [26]).

All participants were informed about the study aims and informed consent was obtained from all participants for the participation in the study. All methods were performed in accordance with the relevant guidelines and regulations by the Ethics Committee of the Chaoyang Hospital.

Consent for publication

Not applicable.

Competing interests

None.

Received: 1 March 2022 Accepted: 4 January 2023

Published online: 13 January 2023

References

- Maglio A, Vitale C, Pellegrino S, Calabrese C, Parente R, Triggiani M, et al. Small airways function: evaluation in a population of adult patients with severe asthma and potential use as a response biomarker for anti-IL5 therapy. Virtual Congress 2020, E-poster session, Number: 2265. 2020. <https://doi.org/10.1183/13993003.congress-2020.2265>.
- Alfieri V, Aiello M, Pisi R, Tzani P, Mariani E, Marangio E, et al. Small airway dysfunction is associated to excessive bronchoconstriction in asthmatic patients. *Respir Res.* 2014;15(1):86–93. <https://doi.org/10.1186/s12931-014-0086-1>.
- Gao J, Wu H, Wu F. Small airway dysfunction in patients with cough variant asthma: a retrospective cohort study. *BMC Pulm Med.* 2021;21(9):49–52.
- Contoli M, Santus P, Papi A. Small airway disease in asthma: pathophysiological and diagnostic considerations. *Curr Opin Pulm Med.* 2015;21(1):68–73.
- Farah CS, et al. Association between peripheral airway function and neutrophilic inflammation in asthma. *Respirology.* 2015;20(6):975–81.
- Huang YJ, Boushey HA. The bronchial microbiome and asthma phenotypes. *Am J Respir Crit Care Med.* 2013;188(10):1178–80.
- Claassen S, et al. The association between faecal microbiota and asthma or wheezing: a systematic review and meta-analysis. *Int J Infect Dis.* 2014;21:336.
- Huang YJ, Nariya S, Harris JM, Lynch SV, Choy DF, Arron JR, Boushey H. The airway microbiome in patients with severe asthma: Associations with disease features and severity. *J Allergy Clin Immunol.* 2015;136(4):874–84.
- Ilmarinen P, Tuomisto LE, Kankaanranta H. Phenotypes, risk factors, and mechanisms of adult-onset asthma. *Mediat Inflamm.* 2015;2015:1–19.
- Bassiri CM, et al. Analysis of the upper respiratory tract microbiotas as the source of the lung and gastric microbiotas in healthy individuals. *Mbio.* 2015;6(2):e00037.
- Huang YJ, Boushey HA. The microbiome in asthma. *J Allergy Clin Immunol.* 2015;135(1):25–30. <https://doi.org/10.1016/j.jaci.2014.11.011>.
- Denner DR, et al. Corticosteroid therapy and airflow obstruction influence the bronchial microbiome, which is distinct from that of bronchoalveolar lavage in asthmatic airways. *J Allergy Clin Immunol.* 2016;137(5):1398–+.
- Durack J, Lynch SV, Nariya S, Bhakta NR, Beigelman A, Castro M, et al. Features of the bronchial bacterial microbiome associated with atopy, asthma, and responsiveness to inhaled corticosteroid treatment. *J Allergy Clin Immunol.* 2017;140(1):63–75.
- Pulmonary Function Workgroup of Chinese Society of Respiratory Diseases (CSR), Chinese Medical Association. The Chinese national guidelines of pulmonary function test. *Chin J Tuberc Respir Dis.* 2014;37:566–71.
- GINA Science Committee, G.B.o.D., GINA Dissemination and Implementation Committee, GINA Executive Director, Asthma management and prevention for adults and children older than 5 years: a pocket guide for health professionals. 2021.
- GINA Science Committee, G.B.o.D., GINA Dissemination and Implementation Committee, GINA Executive Director, Global Strategy for Asthma management and Prevention (2021 update). 2021.
- Liu Y, Zhang L, Li HL, Liang BM, Oliver BG. Small airway dysfunction in asthma is associated with perceived respiratory symptoms, non-type 2 airway inflammation, and poor responses to therapy. *Respiration.* 2021;100(8):767–79. <https://doi.org/10.1159/000515328>.
- Ciprandi G, Capasso M, Tosca M, Salpietro C, Salpietro A, Marseglia G, et al. A forced expiratory flow at 25–75% value <65% of predicted should be considered abnormal: a real-world, cross-sectional study. *Allergy Asthma Proc.* 2012;33(1):5–8. <https://doi.org/10.2500/aap.2012.33.3524>.
- Xiao D, Chen Z, Wu S, Huang K, Chen S. Prevalence and risk factors of small airway dysfunction, and association with smoking, in china: findings from a national cross-sectional study. *Lancet Respir Med.* 2020;8(11):1081–93.
- Chanez P, et al. Sputum induction. *Eur Respir J Suppl.* 2002;37(Supplement 37):3s.
- Djukanovic R, et al. Standardised methodology of sputum induction and processing. *Eur Respir J Suppl.* 2002;37(Supplement 37):51s.
- Bokulich NA, et al. Optimizing taxonomic classification of marker-gene amplicon sequences with QIIME 2's q2-feature-classifier plugin. *Microbiome.* 2018;6(1):90.
- Callahan BJ, et al. DADA2: high resolution sample inference from amplicon data. 2015.
- Afgan E, Baker D, Batut B, van den Beek M, Bouvier D, Čech M, et al. The galaxy platform for accessible, reproducible and collaborative biomedical analyses: 2018 update. *Nucleic Acids Res.* 2018;46(Issue W1):W537–W544. <https://doi.org/10.1093/nar/gky379>.

25. Kanehisa M, Furumichi M, Sato Y, Ishiguro-Watanabe M, Tanabe M. KEGG: integrating viruses and cellular organisms. *Nucleic Acids Res*. 2021;49:D545–51.
26. (2020), M.H.e.a., Multivariable Association in Population-scale Meta-omics Studies, <http://huttenhower.sph.harvard.edu/maaslin2>. 2020.
27. Mallick H, R.A., McIver L.J, MaAsLin 2: multivariable Association in Population-scale Meta-omics Studies. R/Bioconductor package, <http://huttenhower.sph.harvard.edu/maaslin2>. 2020.
28. Team R. RStudio: Integrated Development for R. RStudio. Boston: PBC; 2020.
29. Development C. R: a language and environment for statistical computing R Foundation for Statistical Computing. Vienna: R Development Core Team; 2011.
30. Foster Z, Sharpton T, Grunwald N. Metacoder: an R package for visualization and manipulation of community taxonomic diversity data. *Phytopathology*. 2017;107(12):118.
31. Wemheuer, B.a.F, Tax4Fun2: Tax4Fun2: predicting functional profiles from metagenomic 16S rRNA data.. R package version 1.1.5. <https://github.com/bwemheu/Tax4Fun2>. 2020.
32. Kim-Anh Le Cao F.R, Ignacio Gonzalez, Sebastien Dejean, Benoit Gautier, Francois, P.M. Bartolo, Jeff Coquery, FangZou Yao and Benoit Liqueur, mix-Omics: Omics Data Integration Project. R package version 6.1.1. <https://CRAN.R-project.org/package=mixOmics>. 2016.
33. Green B, et al. Pathogenic Bacteria in induced sputum in severe asthma. *Thorax*. 2008;63:A49.
34. Huang YJ, Nariya S, Lynch SV, Harris J, Choy D, Arron JA, Boushey H. The airway microbiome in severe asthma. *J Allergy Clin Immunol*. 2015;136(4):874–84. <https://doi.org/10.1016/j.jaci.2015.05.044>.
35. Goodson JM, Hartman ML, Shi P, Hasturk H, Yaskell T, Vargas J, et al. The salivary microbiome is altered in the presence of a high salivary glucose concentration. *PLoS ONE*. 2017;12(3):e0170437. <https://doi.org/10.1371/journal.pone.0170437>.
36. Sakamoto M, et al. Changes in oral microbial profiles after periodontal treatment as determined by molecular analysis of 16S rRNA genes. *J Med Microbiol*. 2004;53(6):563–71.
37. B, X.W.A. et al., Gut microbiota dysbiosis is associated with Henoch-Schnelein Purpura in children. *Int Immunopharmacol*, 2018. 58: 1–8.
38. Sonnenberg GF, Artis D. Innate lymphoid cell interactions with microbiota: implications for intestinal health and disease. *Immunity*. 2012;37(4):601–10.
39. Pabst and Oliver. New concepts in the generation and functions of IgA. *Nat Rev Immunol*. 2012;12(12):821–32.
40. Larsen JM, Musavian HS, Butt TM, Ingvorse C, Brix S. COPD and asthma-associated Proteobacteria, but not commensal Prevotella spp. promote TLR2-independent lung inflammation and pathology[J]. *Immunology*. 2014;144(2):333–42.
41. Madura LJ, et al. Divergent pro-inflammatory profile of human dendritic cells in response to commensal and pathogenic Bacteria associated with the airway microbiota. *PLoS One*. 2012;7(2):e31976.
42. Rai AK, et al. Dysbiosis of salivary microbiome and cytokines influence oral squamous cell carcinoma through inflammation. *Arch Microbiol*. 2021;203(1):137–52.
43. Shiga Y, Hosomi N, Nezu T, Nishi H, Aoki S, Nakamori M, et al. Association between periodontal disease due to *Campylobacter rectus* and cerebral microbleeds in acute stroke patients. *PLoS ONE*. 2020;15(10):e0239773. <https://doi.org/10.1371/journal.pone.0239773>.
44. Zhu XH, et al. *Campylobacter rectus* infection leads to lung abscess: a case report and literature review. *Infect Drug Resistance*. 2021;14:2957–63.
45. Wang BN, Kraig E, Kolodrubetz D. Use of defined mutants to assess the role of the *campylobacter rectus* S-layer in bacterium-epithelial cell interactions. *Infect Immun*. 2000;68(3):1465–73.
46. Yakob M, et al. *Prevotella nigrescens* and *Porphyromonas gingivalis* are associated with signs of carotid atherosclerosis in subjects with and without periodontitis. *J Periodontol Res*. 2011;46(6):749–55.
47. Gharbia SE, Haapasalo M, Shah HN, Kotiranta A, Lounatmaa K, Pearce MA, Devine DA. Characterization of *Prevotella intermedia* and *Prevotella nigrescens* isolates from periodontic and endodontic infections. *J Periodontol*. 1994;65(1):56–61. <https://doi.org/10.1902/jop.1994.65.1.56>.
48. Shakoar S, et al. *Rothia dentocariosa* endocarditis with mitral valve prolapse: case report and brief review. *Infection*. 2011;39(2):177–9.
49. Kataoka H, Taniguchi M, Fukamachi H, Arimoto T, Morisaki H, Kuwata H. *Rothia dentocariosa* induces tnfr-alpha production in a tlr2-dependent manner. *Pathog Dis*. 2013;71(1):65–8.
50. Ruoff KL. *Streptococcus anginosus* ("Streptococcus milleri"): the unrecognized pathogen. *Clinical Microbiol Rev*. 1988;1:102–8.
51. Mikkelsen H, et al. Interrelationships between colonies, biofilms, and planktonic cells of *Pseudomonas aeruginosa*. *J Bacteriol*. 2007;189(6):2411–6.
52. Green BJ, Wiriyaichaiyorn S, Grainge C, Rogers GB, Kehagia V, et al. Potentially pathogenic airway bacteria and neutrophilic Inflammation in treatment resistant severe asthma. *PLoS ONE*. 2014;9(6):e100645. <https://doi.org/10.1371/journal.pone.0100645>.

Publisher's Note

Springer Nature remains neutral with regard to jurisdictional claims in published maps and institutional affiliations.

Ready to submit your research? Choose BMC and benefit from:

- fast, convenient online submission
- thorough peer review by experienced researchers in your field
- rapid publication on acceptance
- support for research data, including large and complex data types
- gold Open Access which fosters wider collaboration and increased citations
- maximum visibility for your research: over 100M website views per year

At BMC, research is always in progress.

Learn more biomedcentral.com/submissions

